

FORSCHUNGSZENTRUM
ROSSENDORF e.V.

FZR

FZR-61
November 1994

André Thess and Kerstin Nitschke

**A Note on Thermocapillary Instability
in the Presence of a Magnetic Field**

Forschungszentrum Rossendorf e.V.

**Postfach 51 01 19 · D-01314 Dresden
Bundesrepublik Deutschland**

Telefon (0351) 591 2168

Telefax (0351) 591 3484

E-Mail nitschke@fz-rossendorf.de

Contents

0. Abstract	1
1. Introduction	2
2. The stability problem and its exact solution	4
2.1. Governing equations	4
2.2. Solution of the stability problem	10
3. The limit of strong magnetic field	12
3.1. Scaling of the critical parameters	12
3.2. Physical interpretation of the scaling laws	14
3.3. The asymptotic spatial structure of the unstable mode	16
4. Secondary effects	22
4.1. The role of surface deformation	22
4.2. The role of buoyancy force	25
4.3. Thermoelectric effects	26
4.4. Secondary instabilities	28
5. Conclusion and further work	29
6. Acknowledgment	30
7. References	31
8. Critical parameters for onset of Bénard-Marangoni- instability as a function of the Hartmann number	33
9. Captions	34
10. Figures	35

A Note on Thermocapillary Instability in the Presence of a Magnetic Field

André Thess * and Kerstin Nitschke

*Forschungszentrum Rossendorf, Postfach 510119, 01314 Dresden,
Germany*

Abstract

We formulate the asymptotic theory of thermocapillary instability in a planar fluid layer heated from below in the presence of a strong magnetic field corresponding to high Hartmann number. Explicit asymptotic expressions are derived for the velocity perturbation, temperature perturbation and electric current density. Their spatial structure is characterized in terms of Hartmann boundary layers - a concept which permits a physical understanding of more complicated situations involving surface deformation, buoyancy and thermoelectric effects. The physical nature of large scale instabilities in the case of a deformable surface is clarified.

* permanent address:

Institut für Strömungsmechanik, Technische Universität Dresden, 01062 Dresden, Germany

1. Introduction

The temperature-dependence of surface tension constitutes a source for a variety of flow phenomena called thermocapillary effects. Thermocapillary instabilities and thermocapillary convection have received considerable attention due to their appearance in fundamental fluid-dynamical problems such as Rayleigh-Benard instability as well as in applications like crystal growth and metallurgy. An excellent review article of Davis (1987) summarizes the physical aspects of thermocapillarity. The technological need for instability postponement, turbulence suppression and flow control in material processing as well as the seek for low-cost alternatives to space-technologies for crystal growth are currently leading to an increased interest in the interaction between thermocapillary flows in electrically conducting fluids (semiconductor melts, liquid metals) and magnetic fields. While the interplay between *isothermal* flows and magnetic fields is well understood (Moreau 1990), and while a substantial body of literature exists on *buoyancy* driven convection under magnetic field influence (Chandrasekhar 1961) our understanding of *thermocapillary* flow phenomena in the presence of a magnetic field leaves much to be desired.

The aim of the present note is to develop the asymptotic theory of thermocapillary instability for high Hartmann numbers for a simple prototype problem. The problem considered here is a generalization of Pearson's (1958) study of surface tension driven instability in a plane layer of fluid heated from below to an electrically conducting fluid under the influence of a vertical magnetic field. The present problem was first posed by Nield (1966) and later investigated by Maekawa & Tanasawa (1987), Sarma (1983, 1985, 1987) and by Wilson (1993 a,b). The motivation for reconsidering this problem is twofold. Although the values of the critical Marangoni numbers were numerically calculated depending on the strength of the magnetic field, no attempt has been made in the earlier publications to give a physical explanation of the role of the magnetic field and

no analysis has appeared of the spatial structure of the unstable modes which is drastically changed by the magnetic field and which constitutes in integral part of any stability problem involving multiple length scales. The second purpose is to demonstrate the usefulness of an approach to linear stability theory based on symbolic computational rather than on fully numerical evaluation of solutions for problems involving large parameters. Although limited to the class of linear constant coefficient problems, in some cases, like the present one, it is a very efficient method since analytical calculations by hand are too extensive and purely numerical solutions, even if employing highly accurate schemes based on Chebychev polynomials, fail to give meaningful results due to the complicated nested boundary layer structure of the solutions. This type of problem frequently arises in magnetohydrodynamics but also in rotating flows, multiple layer geometries etc.

In the following section we briefly recall the formulation of the stability problem given by Nield (1966) and derive its complete solution. In section 3 we analyze the limiting case of strong magnetic field thereby extracting the basic physical principles partially hidden in the exact solution. Specifically, we derive asymptotic scaling laws for critical parameters and use matched asymptotic expansions for the analysis of the boundary layer structure of the unstable modes. These results provide the rational framework for the understanding of more complicated cases involving surface deformation, buoyancy forces and thermoelectric effects, as detailed in section 4. Finally we give a numerical example for instability postponement by a magnetic field as predicted by the present theory.

It should be mentioned that experimental studies of thermocapillary instabilities in a layer heated from below have not been undertaken yet in the presence of a magnetic field. However, the experiments of Ginde et al (1989) in a layer heated from below (without

magnetic field) and those of Tison et al (1993) in liquid tin layer with magnetic field (heated from the side) are evidence of the progress made in this field.

2. The stability problem and its exact solution

2.1. Governing equations

The system under consideration is sketched in figure 1. A laterally unbounded layer of electrically conducting fluid is confined by a solid wall at $z=0$ and bounded by a free surface at $z=d$. The layer is heated from below and subjected to a homogeneous magnetic field \mathbf{B} . Surface deformations and buoyancy forces are neglected in the canonical problem considered here, although they can have significant influence on the stability results as is discussed in sections 4.1. and 4.2. The decisive ingredient for thermocapillary phenomena is the dependence of surface tension on the temperature, which can be approximated by the linear relationship

$$\sigma = \sigma_0 - \gamma(T - T_0) \quad (2.1)$$

Due to the absence of buoyancy forces this is the only mechanism by which a nonhomogeneous temperature field exerts a force on the fluid. The dynamics of the fluid is governed by the equations

$$\partial_t \mathbf{v} + (\mathbf{v} \cdot \nabla) \mathbf{v} = -\frac{1}{\rho} \nabla p + \nu \Delta \mathbf{v} + \frac{1}{\rho \mu_0} (\nabla \times \mathbf{B}) \times \mathbf{B} \quad (2.2)$$

$$\partial_t T + (\mathbf{v} \cdot \nabla) T = \kappa \Delta T \quad (2.3)$$

$$\partial_t \mathbf{B} + (\mathbf{v} \cdot \nabla) \mathbf{B} = (\mathbf{B} \cdot \nabla) \mathbf{v} + \frac{1}{\mu_0 \sigma_{cl}} \Delta \mathbf{B} \quad (2.4)$$

$$\nabla \cdot \mathbf{v} = 0 \quad (2.5)$$

$$\nabla \cdot \mathbf{B} = 0 \quad (2.6)$$

for the velocity \mathbf{v} , the temperature field T and magnetic field \mathbf{B} . The quantities ρ , ν , μ_0 , κ and σ_{el} are the density, kinematic viscosity, magnetic permeability, thermal diffusivity and electrical conductivity of the fluid, respectively. Eq. (2.4) for the magnetic field is derived from the Maxwell equations (cf. Moreau 1990). For small temperature differences the purely conductive state of the fluid

$$\mathbf{v} = 0, \quad T = T_1 - \beta z, \quad \mathbf{B} = B e_z \quad (2.7)$$

is stable. If the dimensionless Marangoni number

$$Ma = \frac{\gamma \beta d^2}{\rho \kappa \nu} \quad (2.8)$$

exceeds a critical value of approximately 79.6 (Pearson 1958), the system becomes unstable with respect to perturbations having the shape of convection rolls with dimensionless wavenumber $k \sim 1.99$. A sketch of the streamlines is given in fig. 2a. This critical value increases in the presence of a magnetic field (Nield 1966, Wilson 1993a) and is characterized by the dimensionless Hartmann number

$$Ha = Bd \sqrt{\frac{\sigma_{el}}{\rho \nu}} \quad (2.9)$$

Ha^2 is sometimes called Chandrasekhar number Q . In order to distinguish this instability from the classical buoyancy-driven Rayleigh-Bénard instability, we use the terminology Bénard-Marangoni instability. Before presenting the stability analysis, some comments on the choice of the boundary conditions are in order. The source of the instability is the boundary condition at the free surface

$$\rho v \partial_z v_i = \gamma \partial_i T \quad (i = x, y) \quad (2.10)$$

expressing the equality of surface tension gradients and surface shear stress. In the case of different magnetic permeabilities of fluid and adjacent medium one has to add a magnetic term to (2.10) resulting from the linearization of the Maxwellian stress tensor. Moreover we have

$$v_z = 0 \quad (\text{at } z = d) \quad (2.11)$$

and the no slip condition

$$\mathbf{v} = 0 \quad (\text{at } z = 0) \quad (2.12)$$

at the bottom. The bottom is supposed to be an isothermal plate with infinite thermal conductivity and the thermal boundary condition can be written as

$$T(x, y, 0) = T_1 \quad (2.13)$$

The thermal boundary condition at the free upper surface warrants particular attention. Here the heat flux must be equal to the radiative heat loss governed by the Stephan-Boltzmann law. This leads to the boundary condition

$$\lambda_{th} \partial_z T = -ST^4 \quad (2.14)$$

where the universal Stephan-Boltzmann constant $S = 5.67 \cdot 10^{-8} \text{Wm}^{-2}\text{K}^{-4}$ is evaluated in terms of Plancks constant, Boltzmann constant and the speed of light. We have chosen

this condition together with the assumption of vacuum above the fluid because it is the only situation which is free of any *ad hoc* assumptions about the heat transfer across the free surface. Indeed, the frequently used relation

$$\lambda_{th} \partial_z T = -\alpha(T - T_*) \quad (2.15)$$

with T_* being the temperature of an ambient gas is not a boundary condition but rather a definition of a heat transfer coefficient α (see e.g. Landau & Lifshitz 1987). Even for the linearized problem, this coefficient does not only depend on material parameters of the ambient gas but also on the spatio-temporal structure of the velocity and temperature field, i.e. on the wavenumber and frequency. Treating this coefficient as a constant may be justified in engineering applications to get order-of-magnitude estimations but should be avoided in a theory based on first principles. For the basic state equation (2.14) provides the relation $\lambda_{th} \beta = ST^4$ between the surface temperature and the temperature gradient. The continuity of the magnetic field across material boundaries is expressed by

$$[\mathbf{B}] = 0 \quad \text{for } z=0, z=d \quad (2.16)$$

In order to analyze the linear stability of the basic state (2.7) the governing equations are linearized with respect to the perturbations $(\mathbf{v}, \theta, \mathbf{b})$. As shown by Nield 1966, v_z , θ and b_z are the relevant components for the instability. They can be written in normal mode form

$$\begin{aligned} v_z(x, z, t) &= -e^{\lambda t + ikx} W(z) \\ \theta(x, z, t) &= e^{\lambda t + ikx} G(z) \\ b_z(x, z, t) &= e^{\lambda t + ikx} H(z) \end{aligned} \quad (2.17)$$

If there is "exchange of stability" with a mode having $\lambda=0$, we arrive at the following system

$$[(D^2 - k^2)^2 - Ha^2 D^2] W(z) = 0 \quad (2.18)$$

$$(D^2 - k^2) G(z) = W(z) \quad (2.19)$$

with the boundary conditions

$$W(0) = DW(0) = W(1) = D^2W(1) - k^2 Ma G(1) = 0 \quad (2.20a-d)$$

$$G(0) = DG(1) + Bi G(1) = 0 \quad (2.21)$$

Here D is an abbreviation for d/dz , all coordinates are scaled with the layer thickness d , k is the dimensionless wavenumber, and the Biot number Bi is defined as

$$Bi = \frac{4SdT_0^3}{\lambda_{th}} \quad (2.22)$$

The solutions of (2.18)-(2.21) determine the critical Marangoni number as a function of k , Ha and Bi . The Biot number characterizes the heat losses by the free surface. An evaluation of its value for the conditions of the experiments of Ginde et al (1989) (tin at 250°C) leads to a value of about 10^{-2} . For liquid metals at room temperature or slightly above (Mercury, Gallium) this value decreases by another order of magnitude. Therefore we shall consider exclusively the limiting case $Bi=0$, in which the thermal boundary condition at the free surface reduces to

$$DG(1)=0. \quad (2.23)$$

In view of the fact that the basic temperature profile carries a nonzero heat flux it may seem physically inconsistent to require the heat flux of the perturbation to vanish. However, a zero Biot number can always be attained by taking the limit $d \rightarrow 0$ keeping the gradient $\beta = ST_0^4 / \lambda_{th}$ constant. Moreover, it can be shown that for the full problem the first order correction to the Nusselt number for small Bi is

$$Nu = 1 + Bi \langle \theta^0(x, y, z=1) \rangle_{xy} + O(Bi^2) \quad (2.24)$$

and can be calculated from the solution θ^0 of the governing equation with $Bi=0$. Here $\langle \rangle_{xy}$ denotes average over an x-y layer. It should be noted that the magnetic field itself does not appear in the foregoing stability equations. However, for a complete solution of the problem it must be separately determined from the equations

$$(D^2 - k^2) H_b = 0 \quad \text{for } z < 0 \quad (2.25)$$

$$(D^2 - k^2) H = DW \quad \text{for } 0 < z < 1 \quad (2.26)$$

$$(D^2 - k^2) H_t = 0 \quad \text{for } z > 1 \quad (2.27)$$

together with the matching and boundary conditions for the field H_b [H_t] below [on top] of the layer:

$$\begin{aligned} \lim_{z \rightarrow -\infty} H_b &= 0 & \text{for } z \rightarrow -\infty \\ H_b(0) &= H(0), & DH_b(0) &= DH(0) \\ H_t(1) &= H(1), & DH_t(1) &= DH(1) \\ \lim_{z \rightarrow +\infty} H_t &= 0 & \text{for } z \rightarrow +\infty \end{aligned} \quad (2.28)$$

2.2. Solution of the stability problem

With the four roots

$$\begin{aligned}\lambda_{1/2} &= \pm \frac{1}{2} \left(\text{Ha} + \sqrt{\text{Ha}^2 + 4k^2} \right) \\ \lambda_{3/4} &= \mp \frac{1}{2} \left(\text{Ha} - \sqrt{\text{Ha}^2 + 4k^2} \right)\end{aligned}\tag{2.29}$$

of the characteristic equation of (2.28) the solution for the velocity can be written as

$$W(z) = \sum_{i=1}^4 w_i e^{\lambda_i z}\tag{2.30}$$

The four unknown coefficients are determined by the four boundary conditions (2.20). Only one of these boundary conditions contains the unknown temperature perturbation $G(1)$. However, due to the linearity of the problem, we can give $G(1)$ an arbitrary nonzero value; we chose $G(1)=1/(\text{Ma } k^2)$ as a particularly convenient gauge. With the coefficients w_i , the solutions to the equations (2.19) and (2.28) are readily derived as

$$\begin{aligned}G(z) &= \sum_{i=1}^4 \frac{w_i e^{\lambda_i z}}{\lambda_i^2 - k^2} + g_+ e^{+kz} + g_- e^{-kz} \\ H(z) &= \sum_{i=1}^4 \frac{w_i \lambda_i e^{\lambda_i z}}{\lambda_i^2 - k^2} + h_+ e^{+kz} + h_- e^{-kz} \\ H_b(z) &= h_b e^{+kz} \\ H_t(z) &= h_t e^{-kz}\end{aligned}\tag{2.31}$$

The six coefficients g_+ , g_- , h_+ , h_- , h_b , h_t are determined by the six boundary conditions (2.21), (2.23), (2.28). The explicit expression for the neutral curve $\text{Ma}(k, \text{Ha})$ is obtained by calculating $G(1)$ and requiring that $G(1)=1/(\text{Ma } k^2)$ as assumed above.

This leads to the following explicit expression for the critical Marangoni number as a function of the wavenumber k and of the Hartmann number Ha .

$$\begin{aligned}
 Ma = & \left\{ 2Ha^2 \cosh(k) \left[(Ha^2 + 4k^2) \sinh(Ha) - Ha \sqrt{Ha^2 + 4k^2} \sinh(Ha^2 + 4k^2) \right] \right\} / \\
 & [(Ha^2 + 4k^2) [\sinh(Ha - k) + \sinh(Ha + k)] - 4Hak \sinh(k) \\
 & + 2 \left(Ha^2 + 4k^2 + Ha \sqrt{Ha^2 + 4k^2} \right) \sinh(\lambda_3) + 2 \left(-Ha^2 - 4k^2 + Ha \sqrt{Ha^2 + 4k^2} \right) \sinh(\lambda_1) \\
 & + \left(2Hak + Ha \sqrt{Ha^2 + 4k^2} \right) \sinh \left(k - \sqrt{Ha^2 + 4k^2} \right)]
 \end{aligned}
 \tag{2.32}$$

Extensive use has been made of the symbolic computation capabilities of *Mathematica* (Wolfram 1991) in the derivation of the explicit expressions of the unknown coefficients, and in the expression of the neutral curve as well as in the evaluation of the limiting case $Ha \rightarrow \infty$. Most expressions shall not be given here due to their length although they are readily available.

For a fixed Ha (fixed magnetic field), Ma gives the Marangoni number at which a perturbation with wavenumber k becomes unstable. In the limit $Ha \rightarrow 0$ the curve converges to that of the nonmagnetic problem calculated by Pearson (1958) with the minimum $Ma_c = 79.61$ at $k_c = 1.993$. The Marangoni number for each k -value is a monotonically increasing function of Ha indicating the stabilizing influence of the magnetic field. The points $k_c(Ha)$ at which the Marangoni number attains its minimum $Ma_c(Ha)$ determine the threshold of the Marangoni instability onset and the wavelength of the first unstable mode. Their values are listed in table 1. The values agree with those numerically calculated by Nield (1966) and Wilson (1993b). High accuracy can be obtained by using the exact solution in conjunction with high precision arithmetic in order to evaluate exponentials with increments as high as 10^6 .

From the foregoing results it is possible to reconstruct the velocity, temperature and magnetic field associated with the first unstable mode for arbitrary Hartmann number. In fig. 2 we depict the changes of the streamlines of the unstable mode under the influence of the magnetic field. In the nonmagnetic case the lateral size of the unstable rolls is of the same order as the layer thickness. For increasing values of the magnetic field the lateral distance between adjacent cells decreases and their centers shift towards the free surface. In the limit $Ha \rightarrow \infty$ the hydrodynamic behaviour and the size of unstable perturbations is governed by simple laws that are extracted from the exact solution in the next section.

3. The limit of strong magnetic field

3.1. Scaling of the critical parameters

In many magnetohydrodynamic problems a deeper physical understanding can be gained by considering the limit of strong magnetic field ($Ha \rightarrow \infty$) even though the magnitude of Ha in typical applications rarely exceeds 10^3 . Let us first use expression (2.32) to derive the asymptotic dependence of the critical Marangoni number on Ha . If we use symbolic computation packages to attempt to calculate the limit of Ma for $Ha \rightarrow \infty$ or if we use the Taylor expansion around $1/Ha = 0$ we fail partially because Ma tends to infinity and partially since the analytic structure of the function $Ma(k, Ha)$ in the vicinity of $1/Ha=0$ is singular. In order to evaluate the limiting behaviour we make the substitutions

$$\begin{aligned} \mathcal{M}a &= \frac{Ma}{Ha^2} \\ \kappa &= \frac{k}{Ha^{1/2}} \end{aligned} \tag{3.1}$$

which already incorporate scaling laws anticipated from the behaviour of the numerical values in table 1. Taking the limit $Ha \rightarrow \infty$ then provides the following result to leading order in $1/Ha$

$$\mathcal{M}a = 1 + \ell^2 \frac{2\kappa e^{2\kappa^2}}{e^{2\kappa^2} - 1} + O(Ha^{-1}) \quad (3.2)$$

with

$$\ell = \frac{1}{Ha^{1/4}} \quad (3.3)$$

Equation (3.2) was first derived by Wilson (1993a) using a different method. From (3.2) we conclude that $\mathcal{M}a$ and κ are the relevant stability parameters in the limit of strong magnetic field instead of Ma and k . The asymptotic neutral curve $\mathcal{M}a(\kappa)$, represented in fig. 3, is then the magnetic counterpart to the result of Pearson (1958).

$\mathcal{M}a(\kappa)$ has a minimum at the solution $\kappa_c = 0.792601$ of the transcendental equation $\exp(2\kappa^2) - 4\kappa^2 - 1 = 0$ at which it takes a value of $\mathcal{M}a_c = 1 + 2.21604 \ell^2$. In the vicinity of this minimum $\mathcal{M}a(\kappa)$ has a parabolic shape with a curvature proportional to $1/\ell$. It follows from the foregoing results that the critical Marangoni number and wavenumber scale as

$$\begin{aligned} Ma_c &= \mathcal{M}a_c Ha^2 = Ha^2 \left(1 + \frac{2.21604}{Ha^{1/2}} + O(Ha^{-1}) \right) \\ k_c &= \kappa_c Ha^{1/2} = 0.792601 Ha^{1/2} \end{aligned} \quad (3.4)$$

The quantity ℓ , usually called the correlation length, can be interpreted as a characteristic length scale over which spatial modulations of the basic periodic pattern can occur in the

weakly nonlinear regime slightly above the instability threshold (Manneville 1991). Above instability threshold the term $\beta^2(\kappa - \kappa_c)^2$ is of the order of one implying that superposition of unstable modes from the band with $\Delta\kappa \sim 1/l$ and therefore with modulation length l can occur.

3.2. Physical interpretation of the scaling laws

The basic instability mechanism is independent of the magnetic field. Consider a local hot spot that has arisen at the surface due to a small temperature fluctuation. Heat conduction tends to smooth out the spot, whereas thermocapillarity (cf. eq. 2.10) produces a radially outward flow above the spot which, by continuity, causes a vertical upflow to transport new hot fluid to the surface. Both mechanisms counteract, and for sufficiently large temperature gradients, thermocapillary shear production ultimately dominates thermal diffusion and viscous dissipation. In the absence of the magnetic field the surface shear associated with a velocity v_x is of the order v_x/d . It follows from the continuity equation that v_z is of the same order as v_x since the wavenumber of the most unstable perturbations is of the order of one for the nonmagnetic problem. The vertical velocity perturbation causes a surface temperature perturbation

$$\Delta T_{\text{surface}} \sim \left(\frac{v_z d}{\kappa} \right) \Delta T \sim \left(\frac{v_x d}{\kappa} \right) \Delta T \quad (3.5)$$

Inserting this estimate into the Marangoni boundary condition (2.10) which expresses the balance between shear and thermocapillary forces, gives the result $Ma \sim 1$ expressing that the Marangoni number is the pertinent instability parameter.

In the presence of the magnetic field these estimates have to be modified only in one respect. As for other magnetohydrodynamic flows, the effect of a transverse magnetic

field is to damp the horizontal component everywhere except in narrow boundary layer (Hartmann layer) with thickness

$$\delta \sim \frac{d}{Ha} \quad (3.6)$$

in which viscous forces are of the same order as electromagnetic forces (Lorentz forces) resulting from the interaction of the magnetic field with the electric current induced by the fluid motion (cf. fig. 2a). Consequently, the foregoing considerations have to be repeated with δ taken as the relevant length scale of the problem instead of d . A velocity perturbation v_x produces shear

$$\partial_z v_x \sim Ha \frac{v_x}{d} \quad (3.7)$$

From the continuity equation and from the scaling law of the wavenumber we conclude that

$$v_z \sim \frac{v_x}{Ha^{1/2}} \quad (3.8)$$

and

$$\Delta T_{\text{surface}} \sim \left(\frac{v_z \delta}{\kappa} \right) \Delta T \sim \left(\frac{v_x d}{\kappa} \right) \frac{\Delta T}{Ha^{2/3}} \quad (3.9)$$

Again equating shear stress and thermocapillary stress in equation (2.10) leads to the result

$$\frac{Ma}{Ha^2} \sim 1 \quad (3.10)$$

in agreement with the exact result that Ma governs the instability.

3.3. The asymptotic spatial structure of the unstable mode

In principle, the exact solution for $W(z)$, $G(z)$ and $H(z)$ immediately provides us with all physical quantities including the vorticity

$$\omega_y(x, z) = -\frac{i}{k} e^{ikx} (D^2 - k^2) W(z) \quad (3.11)$$

and the electric current density

$$j_y(x, z) = +\frac{i}{k} e^{ikx} (D^2 - k^2) H(z) = \frac{i}{k} e^{ikx} DW(z) \quad (3.12)$$

parallel to the axis of the rolls. Nevertheless, we shall independently derive the limiting behaviour of $W(z)$ by matched asymptotic expansion since this method provides better insight into the boundary layer structure of the flow field.

The method of matched asymptotic expansion, thoroughly described by Nayfeh (1981), has been successfully applied to other magnetohydrodynamic problems (see e.g. Hunt & Shercliff 1971, Hunt & Ludford 1968). Therefore we shall omit all technical details and present only the main steps. For the solution of the system (2.18), (2.19), (2.20) and (2.23) in the limit $Ha \rightarrow \infty$ we split the interval $[0, 1]$ in three regions: the bottom layer $0 < z \leq \delta$, the core $\delta < z < 1 - \delta$ and the surface layer $(z-1) \leq \delta$ with $\delta = 1/Ha$. Quantities referring to each region are denoted by subscripts b , c and s . Setting $k = \kappa Ha^{1/2}$ and $Ma = \mathcal{M}a Ha^2$ we obtain to leading order in the Hartmann number the equation for the core velocity

$$(D^2 - \kappa^2)W_c = 0 \quad (3.13)$$

with the general solution

$$W_c(z) = c_1^{(c)}e^{\kappa^2 z} + c_2^{(c)}e^{-\kappa^2 z} \quad (3.14)$$

Within the bottom layer the velocity rapidly decreases to zero in order to satisfy the no-slip condition. To resolve the boundary layer we introduce the stretched coordinate

$$\zeta = \text{Ha } z, \quad D = \text{Ha } D_\zeta \quad (3.15)$$

The leading order equation in the bottom layer and the corresponding solution becomes

$$(D_\zeta^4 - D_\zeta^2)W_b(z) = 0 \quad (3.16)$$

whence

$$W_b(\zeta) = c_0^{(b)} + c_1^{(b)}\zeta + c_2^{(b)}e^\zeta + c_3^{(b)}e^{-\zeta} \quad (3.17)$$

The requirement that W must remain finite in the limit $\zeta \rightarrow \infty$ together with the boundary conditions (2.20 a,b) determines three of the unknown parameters

$$c_2^{(b)} = 0, \quad c_3^{(b)} = -c_0^{(b)}, \quad c_1^{(b)} = -c_0^{(b)} \quad (3.18)$$

in terms of the fourth one. Analogous assumptions apply for the surface layer with the coordinate $\zeta = \text{Ha}(1-z)$ and $D = -\text{Ha } D_\zeta$. The corresponding expressions are

$$(D_\zeta^4 - D_\zeta^2)W_s(z) = 0 \quad (3.19)$$

$$W_s(\zeta) = c_0^{(s)} + c_1^{(s)}\zeta + c_2^{(s)}e^\zeta + c_3^{(s)}e^{-\zeta} \quad (3.20)$$

From the boundary conditions (2.20 c,d) it follows that

$$c_2^{(s)} = 0, \quad c_0^{(s)} = -c_3^{(s)} = -Ha \xi^2 Ma G(1) \quad (3.21)$$

According to the procedure of matched asymptotic expansion the remaining unknown coefficients

$$c_1^{(c)}, c_2^{(c)}, c_0^{(b)}, c_1^{(i)} \quad (3.22)$$

are determined from the matching condition. This condition requires the outer expansion of the boundary layer solution to be equal to the inner expansion of the core solution. More precisely, the boundary layer solutions (3.17) and (3.20) in the limit $\zeta \rightarrow \infty$

$$\begin{aligned} W_{bc} &= c_0^{(b)} + c_1^{(b)}\zeta \\ W_{sc} &= c_0^{(s)} + c_1^{(s)}\zeta \end{aligned} \quad (3.23)$$

must be equated to the core solution

$$\begin{aligned} W_{cb} &= w_0^{(cb)} + w_1^{(cb)}\zeta \\ W_{cs} &= w_0^{(cs)} + w_1^{(cs)}\zeta \end{aligned} \quad (3.24a,b)$$

expanded in the vicinity of $z=0$ and $z=1$, respectively. The wall coordinates in these equations refer to different regions. This leads to the 4 matching conditions

$$c_{0/1}^{(b)} = w_{0/1}^{(cb)}, \quad c_{0/1}^{(s)} = w_{0/1}^{(cs)} \quad (3.25)$$

All the w -coefficients can be expressed in terms of the unknown coefficients which are therefore uniquely determined. A composite solution, i.e. a solution uniformly approximating the solution over the whole interval $[0,1]$ can be obtained by adding to the core solution the difference between the core- and the boundary layer solutions

$$W(z) = \Delta W_b + W_c + \Delta W_s \quad (3.26)$$

which leads to the final result

$$W(z) = Ha \mathcal{M}a G(1) \left\{ \frac{\kappa^4 \cosh(\kappa^2 z) - Ha \kappa^4 \sinh(\kappa^2 z) - \kappa^4 e^{-Ha z}}{Ha \sinh(\kappa^2) - \kappa^2 \cosh(\kappa^2)} + \kappa^2 e^{-Ha(1-z)} \right\} \quad (3.27)$$

The function $W(z)$ is plotted in figure 4a for $Ha=100$ together with that for a lower value of Ha . In this figure we see that the vertical component increases monotonically in the core and decreases to zero within the Hartmann boundary layer. Equation (3.27) clearly reveals the boundary layer structure of the solution. The first terms depending on the "slow" coordinate κz describe the core solution, the exponential terms containing Ha describe the boundary layers. The correctness of the formula has been checked by comparison with the exact result. Fig. 4b shows the behaviour of the vertical velocity component which is obtained by differentiation of W . It is strongly affected by the magnetic field in contrast to v_z because the induced electric current

$$\mathbf{j} = \sigma(\mathbf{E} + \mathbf{v} \times \mathbf{B}) \quad (3.28)$$

produces a Lorentz force opposite to the v_x . The v_z component is not directly affected since it is parallel to the applied magnetic field. The profile of the electric current is identical to DW (cf. equation 2.26).

Now we turn to the evaluation of the asymptotic temperature profile. It turns out that the above procedure cannot be carried out in the same way as for $W(z)$. The leading order core solution for the temperature $G_c(z) = -W_c(z)/k^2 Ha$ is uniquely determined by the velocity field and contains no undetermined coefficients. The surface layer solution contains two free coefficients. There are however three conditions to be satisfied, namely continuity of temperature G and heat flux DG between the core solution and the surface layer solution as well as the zero heat flux boundary condition $DG=0$ at the free surface. It is clear that these three conditions cannot be satisfied by only two parameters and therefore higher order terms must be included into the analysis. Fortunately, this can be circumvented by calculating first the exact solution

$$G(z) = Ma G(1) \left\{ \frac{Ha [Ha \sinh(\kappa^2 z) - \kappa^2 \cosh(\kappa^2 z)] - \kappa^2 e^{-Ha z}}{[Ha \sinh(\kappa^2) - \kappa^2 \cosh(\kappa^2)](Ha^2 - \kappa^2)} + \frac{\kappa^2 e^{-Ha(1-z)}}{(Ha^2 - \kappa^2)} \right\} + d_1 e^{-\kappa \sqrt{Ha}(1-z)} + d_2 e^{+\kappa \sqrt{Ha}(1-z)} \quad (3.29)$$

of equation (2.19) with W taken from (3.27) and systematically removing higher order terms of $1/Ha$ except those necessary to satisfy the boundary condition. We note that the solution of the inhomogeneous equation is of the order $Ma G(1) O(1)$ in the core. In the bottom layer the order of magnitude of G is $Ma G(1) O(Ha^{-1})$ i.e. the boundary condition at the bottom is fulfilled to leading order of the Hartmann number and the coefficient d_2 is zero in this approximation. The coefficient d_1 , however, is necessary to satisfy the free surface boundary condition which is violated by the inhomogeneous term in (3.29) to the order of $Ma G(1) O(1)$. The result for d_1 is

$$d_1 = \frac{\mathcal{M}a G(1) \kappa}{\sqrt{\text{Ha}}} \left(\frac{\cosh(\kappa^2)}{\sinh(\kappa^2)} + 1 \right) \quad (3.30)$$

With this step done we can write down the final expression for the temperature field in the limit $\text{Ha} \rightarrow \infty$ as

$$G(z) = \mathcal{M}a G(1) \left\{ \frac{\sinh(\kappa^2 z)}{\sinh(\kappa^2)} + \frac{\kappa^2 e^{-\text{Ha}(1-z)}}{\text{Ha}} - \frac{2\kappa e^{2\kappa^2}}{\text{Ha}^{1/2} (e^{2\kappa^2} - 1)} e^{-\kappa \sqrt{\text{Ha}}(1-z)} \right\} \quad (3.31)$$

The correctness of the approximations (3.29) and (3.31) is revealed by calculating the critical curve $\mathcal{M}a(\kappa)$ from the requirement that the rhs. of eq. (3.31) at $z=1$ be equal to $G(1)$. Surprisingly, the result

$$\mathcal{M}a = 1 + \frac{1}{\text{Ha}^{1/2}} \frac{2\kappa e^{2\kappa^2}}{e^{2\kappa^2} - 1} + O(\text{Ha}^{-1}) \quad (3.32)$$

does not only give the correct asymptotic scaling (3.4) but is *identical* to the exact asymptotic neutral curve. Figure 4c shows the temperature profile calculated from (3.32). Although not seen in the figure, the thermal perturbations consist of two nested boundary layers - one with thickness $\delta \sim 1/\text{Ha}$ is due to the advection by the velocity perturbation, the second boundary layer with $\delta \sim 1/\text{Ha}^{1/2}$ is due to the thermal boundary condition. The asymptotic scaling regime is reached when $\text{Ha}^{1/2} \gg 1$ which is likely to be the reason for the failure of Nield's (1966) numerical method to give correct scaling results for high Ha .

4. Secondary effects

The results of the foregoing section can be used to physically understand more complicated situations obtained from our canonical problem by

- (i) allowing for surface deflection,
- (ii) adding buoyancy forces,
- (iii) including thermoelectric effects that could occur at the interface between the electrically conducting fluid and the bottom material having in general a nonzero electrical conductivity.

In the following we shall briefly provide a physical explanation of previous results (Wilson 1993 a,b) on the influence of surface deflection and of buoyancy forces from the viewpoint of our asymptotic theory. Moreover we shall assess the importance of thermoelectric effects for moderate Hartmann numbers. The latter problem has never been considered, although it is important for experimental studies.

4.1. The role of surface deformation

It was shown by Scriven & Sternling (1964) that the stability properties are significantly changed in the long wave limit if the constraint of a non-deformable surface is released. More precisely, in the limit $k \rightarrow 0$ the critical Marangoni number does not tend to infinity as in the case of an undeformed surface. Instead, it tends to zero as

$$\text{Ma} \sim \frac{k^2}{C} \tag{4.1}$$

in the absence of gravity ($g=0$), and it converges to a constant

$$\text{Ma} \sim \frac{\text{Bo}}{C} \quad (4.2)$$

if gravity is present. Here $C = \rho\nu\kappa / \sigma_0 d$ and $\text{Bo} = \rho g d^2 / \sigma_0$ denote respectively the Capillary number and the Bond number, and σ_0 is the surface tension. It is worth noting that the physical mechanism of these instabilities is quite different from the instabilities at intermediate wavenumbers in that the threshold of the long wave instabilities does not depend on the molecular transport coefficients ν and κ . Therefore the use of Marangoni number, containing both ν and κ , is somewhat misleading in this case. This is seen if we transform equations (4.1) and (4.2) back to physical variables, which gives

$$\gamma\beta \sim \sigma d k^2 \quad (4.3)$$

for $g=0$ and

$$\gamma\beta \sim \rho g d \quad (4.4)$$

for nonzero g . Recall that β is the critical temperature gradient. Equations (4.3) and (4.4), neither of which contains ν or κ , lead to the somewhat surprising conclusion that the long wave instabilities would occur no matter how large the viscosity of the fluid is, i.e. even in the case $\nu \rightarrow \infty$. This paradox is resolved by noting that although ν and κ do not determine the instability threshold, they do enter into the growth rate, which tends to zero as $\nu \rightarrow \infty$. Therefore care must be taken in predicting long wave instabilities for experimental situations without analyzing their growth rate, which may be so slow that the instability is not observable in a laboratory experiment because the characteristic time scale is exceedingly large.

The instability mechanism itself can be understood without reference to thermal diffusion. Before discussing the magnetic case, it is worth explaining the nonmagnetic long wave instability mechanism by a simple gedanken experiment, which unfortunately was never made in previous publications. Consider a hypothetic system in which the temperature is always equal to the unperturbed distribution $T = -\beta z$, even if the velocity is nonzero. Such a case obviously corresponds to infinite thermal conductivity. If the planar shape of the upper surface is perturbed by a bump δz , the temperature at the top of the perturbation differs by $\delta T = -\beta \delta z$ from the other points of the free surface. This temperature difference creates a thermocapillary flow towards the bump and, as a result, its height increases. Obviously, the mere existence of such an instability mechanism is not related to viscosity, which only determines the magnitude of the thermocapillary velocity and thereby the growth rate of instability. The question why the instability for $g=0$ can occur for arbitrarily small temperature gradients, while a finite temperature gradient is necessary in the presence of gravity, can be understood by an energetic argument. At zero gravity the instability must only perform mechanical work against surface energy. Since the energy of a deformed surface tends to zero as $k \rightarrow 0$, surface deformation does not provide an efficient mechanism for instability saturation. In contrast, for nonzero gravity a finite amount of energy is necessary to overcome the potential energy of the difference between a deformed and a nondeformed surface, and the critical temperature gradient is finite.

Let us analyze the influence of a magnetic field on the long wave instabilities. The magnetic field affects only molecular transport processes since it gives rise to Joule energy dissipation. It does not affect surface energy or potential energy which are responsible for the saturation of the long wave instability as discussed above. Therefore we can conclude that the magnetic field does not have any significant influence on the instability thresholds but it does have influence on the growth rates. This is confirmed by

the results of Wilson (1993a,b) who finds that in the limit of strong magnetic field relations (4.1) and (4.2) still hold, although with numerical factors differing from the nonmagnetic case. The action of the magnetic field consists of two counteracting elements. On the one hand, a strong magnetic field will confine the flow to the Hartmann boundary layer $\delta \sim 1/Ha$ in the immediate vicinity of the free surface. Equations (4.3) and (4.4) show that a reduced effective layer thickness amounts to a decrease of the critical temperature gradient. On the other hand, the Maxwellian stress due to the magnetic field enters into the normal stress boundary conditions and inhibits surface deflections. Both mechanisms counteract and compensate each other in the limit of high Hartmann numbers, thus leading to unchanged scaling properties of the instability thresholds. We note, parenthetically, that the incorrect result of Sarma (1983, 1985, 1987) of an asymptotically decreasing critical temperature gradient can be easily understood from the foregoing considerations. Sarma (1983, 1985, 1987) did not include the magnetic term into the boundary condition. His results reflect the destabilizing influence of the reduced effective layer thickness but do not contain the stabilization due to the magnetic term in the normal stress boundary conditions.

Since the presence of a strong magnetic field adds an additional mechanism of energy dissipation, it is clear that the growth rates of the long wave instability tends to zero as $Ha \rightarrow \infty$. Our asymptotic method can be used to investigate the asymptotic behaviour of the growth rates, which would be important for practical purposes.

4.2. The role of buoyancy force

In the absence of capillary forces buoyancy leads to the classical Rayleigh-Bénard instability in which the critical Rayleigh number and the wavenumber scale as $Ra \sim Ha^2$ and $k \sim Ha^{1/3}$ for strong magnetic fields (Chandrasekhar 1961). Nield (1964) and Wilson (1993 b) have studied the interplay between buoyancy and surface tension in the presence

of a magnetic field calculating the Marangoni number as a function of Ra and Ha . As a general result, the coupling between both effects is found to be weakened by the magnetic field. This is exemplified by the fact that the slope of the curve of the critical Marangoni number versus the critical Rayleigh number decreases in the limit of $Ha \gg 1$ in the vicinity of $Ra=0$. This result can be easily interpreted in terms of Hartmann boundary layers. In a strong magnetic field the action of the thermocapillary forces is entirely confined to the Hartmann layer below the free surface, whereas the buoyancy forces still act in the whole core. Thus, both mechanisms become increasingly separated as the Hartmann boundary layer thickness tends to zero. For small Rayleigh numbers, such as relevant for experimental studies in shallow layers, the method of matched asymptotic expansion can be generalized to the presence of buoyancy by retaining the boundary layer equations (3.16) and (3.19) while taking into account the buoyancy term in the equation (3.13) for the core velocity.

A comment is in order on the possibility of reducing the influence of buoyancy. Apart from microgravity experiments in space and experiments in shallow layers, there is a third way to eliminate the influence of gravity. It is known that in certain Ga-Sn alloys the surface *increases* with temperature (Bojarevics 1993). This implies that the thermocapillary instability manifests itself if the fluid is heated from *above*. This case is stable from the viewpoint of buoyancy, and thermocapillarity is the only destabilizing force.

5.3. Thermoelectric effects

Thermoelectric effects arise at non-isothermal boundaries between two electrically conducting materials such as a liquid metal and solid bottom material in a Marangoni experiment. These thermoelectric currents add to the currents induced by the motion of fluid in the magnetic field and can lead to significant changes of flows. Let us estimate

the ratio between thermoelectric currents and currents induced by the velocity field for small Hartmann numbers referring the reader to the work of Shercliff (1979) for the general theory of thermoelectric magnetohydrodynamics. At the interface between two metals an tangential electric current density

$$j_{te} \sim \frac{\sigma_{el} \Delta S \Delta_i T}{d} \quad (4.5)$$

is generated where $\Delta_i T$ is a temperature variation along the interface over the distance d . If the bottom is an ideal heat conductor and therefore isothermal, as assumed in our theory, no thermoelectric currents can occur. In a bottom with finite but high thermal diffusivity κ_b , however, a fraction

$$\Delta_i T \sim \frac{\kappa}{\kappa_b} \Delta_{ii} T \quad (4.6)$$

of the transverse core temperature difference can penetrate the interface. Recalling the relation (3.5) $\Delta_{ii} T$ can be expressed as a function of the perturbation velocity and the thermoelectric current can be estimated as

$$j_{te} \sim \frac{\sigma v_z}{\kappa_b} \Delta S \Delta T \quad (4.7)$$

the ratio of this current to the velocity induced electric current

$$j_v \sim \sigma v_x B \quad (4.8)$$

is

$$\frac{j_{te}}{j_v} \sim \frac{\Delta S \Delta T}{B \kappa_b} \quad (4.9)$$

Thus, thermoelectric currents become important for weak magnetic fields. For $\Delta T=1\text{K}$, $\kappa_b=1.17 \cdot 10^{-4}\text{m}^2/\text{s}$ (copper), $B=0.1$ Tesla, and $\Delta S=6\mu\text{V/K}$ (copper-mercury) this ratio is roughly 0.5, i.e. thermocapillary forces are as important as purely electromagnetic ones. Thermoelectric currents are in the same plane as the velocity perturbation and their interaction with the vertical magnetic field creates a force with a nonzero y -component. The stability problem becomes thus three-dimensional in the presence of thermoelectricity.

4.4. Secondary instabilities

Above instability threshold the nonlinear terms in the governing equation lead to a saturation of the primary instability. Linear stability theory cannot predict the selected pattern, but preliminary results of direct numerical simulations of the full three-dimensional system of equations show the formation of hexagonal cells. Since the thickness of the Hartmann layer decreases faster than the critical wavelength, the aspect ratio of the convective cells becomes very large. Locally the flow tends to be parallel with the velocity depending primarily on z and the induced temperature gradient being parallel to the surface. This situation is locally very similar to that of a planar layer heated from the side as considered by Smith & Davis (1983). Smith and Davis found that low Prandtl number convection is susceptible to perturbations having the form of hydrothermal waves. It is likely that this kind of instabilities will arise as a secondary instability of the established convection pattern leading to time-dependence.

5. Conclusions and further work

We have established the asymptotic theory of thermocapillary instability in the limit of strong magnetic field. The main results of the work are

- (i) a rigorous derivation of the asymptotic scaling laws (3.4) for the critical parameters describing the postponement of Benard-Marangoni instability by a strong magnetic field,
- (ii) explicit asymptotic expressions for the profile of the perturbation velocity (3.27), temperature (3.29), and electric current density,
- (iii) the physical interpretation of the stability properties in terms of well established magnetohydrodynamic principles.

To the best knowledge of the authors, no experiments have been performed yet on the suppression of Benard-Marangoni instability by a magnetic field. However, the continuing experimental efforts (Ginde 1989, Tison 1993) make such results likely to appear in the foreseeable future and we shall give a numerical example how the present theory translates into experimental parameters. Assuming a Gallium layer with $d=1\text{mm}$ the following critical temperature difference and wavelength are obtained

$B = 0 \text{ Tesla}$ ($Ha=0$)	$\Delta T_c = 23 \text{ K}$	$\lambda_c = 3.2 \text{ mm}$
$B = 0.1 \text{ Tesla}$ ($Ha=5$)	$\Delta T_c = 40 \text{ K}$	$\lambda_c = 2.6 \text{ mm}$

It is noteworthy that the instability postponement is remarkable even for moderately strong magnetic fields.

We have investigated the case in which both the temperature gradient and the magnetic field have the same direction and are perpendicular to the free fluid surface.

Generalizations are necessary in order to cope with practical applications such as crystal growth. Technological problems involve temperature gradients with nonzero components of temperature gradients parallel *and* perpendicular to the fluid. The parallel component of the temperature gradient generates a basic flow which may be stable or unstable depending on temperature and magnetic field. This problem has been solved by Smith and Davis 1983 for the nonmagnetic problem. The investigation of this stability problem with magnetic fields is presently underway and will be reported elsewhere.

Acknowledgment

This work is supported by Deutsche Forschungsgemeinschaft under Grant number Th 497/2-1. The authors are pleased to acknowledge fruitful discussions with J. Priede, Y. Gelfgat, G. Gerbeth, A. Bojarevics and V. Galindo.

References

- Bojarevics A., 1993
private communication
- Chandrasekhar S., 1961
Hydrodynamic and Hydromagnetic Stability, Clarendon Press, Oxford
- Davis S.H., 1987
Ann. Rev. Fluid Mech., vol 19, 403-435
- Ginde R.M., Gill W.N., Verhoeven J.D., 1989
Chem. Engin. Comm. , vol. 82, 223-228
- Hunt J.C.R., Ludford G.S.S., 1968
J. Fluid Mech., vol. 33, 775-801
- Hunt J.C.R., Shercliff J.A., 1971
Ann. Rev. Fluid Mech., vol 3, 37
- Landau L.D., Lifshitz E.M., 1987
Course of Theoretical Physics, Volume 6 - Fluid Mechanics, Pergamon Press,
New York
- Maekawa T, Tanasawa I, 1987
Int. J. Heat Mass transfer, vol. 32 (7), 1377-1380
- Manneville P., 1991
Structures dissipatives, chaos et turbulence, Collection Alea Saclay,
- Moreau R., 1990
Magnetohydrodynamics, Kluwer Academic Publisher, Dordrecht
- Nayfeh A.H., 1981
Introduction to perturbation techniques, Wiley & Sons, New York
- Nield D.A., 1966
Zeitschr. angew. Math. und Physik, vol. 17, 131-139

Nitschke K., Thess A., Gerbeth G., 1992

in: *Microgravity Fluid Mechanics, Proceedings of the IUTAM Symposium
Bremen 1991*, ed. H.J. Rath, p. 285-296, Springer Verlag Berlin

Pearson J.R., 1958

J. Fluid Mech., vol 4, 489-500

Sarma G.S.R., 1983

Adv. Space. Res., vol. 3, 33-36

Sarma G.S.R., 1985

PhysicoChem. Hydrodynamics, vol. 6, 283-300

Sarma G.S.R., 1987

J. Thermophys., vol. 1, 129-135

Shercliff J.A., 1979

J. Fluid Mech., vol. 91, 231-251

Smith M.C., Davis S.H., 1983

J. Fluid Mech. vol. 132, 119-144

Tison P, Camel D., Favier J., 1993

Preprint CEA/DTA/CEREM/DEM, Grenoble

Wilson S. K., 1993a

Q. J. Appl. Math., vol. 46, 211-248

Wilson S. K., 1993b

J. Engin. Math., vol. 27, 161-188

Wolfram S., 1991

Mathematica, Addison Wesley, Redwood City

Table 1: Critical parameters for onset of Benard-Marangoni-instability as a function of the Hartmann number

Ha	Ma _c	k _c
0.001	79.6064	1.9929
0.01	79.6070	1.9929
0.1	79.6325	1.9931
1	82.1724	2.0147
10	284.222	2.9590
100	12830.2	8.0924
1000	1.07532 10 ⁶	25.116
10000	1.02266 10 ⁸	79.276
100000	1.00706 10 ¹⁰	250.64

Captions

Fig. 1: Sketch of the geometry of the fluid layer

Fig. 2: Sketch of the streamlines of unstable modes. (a) for the non-magnetic problem, (b) a strong magnetic field corresponding to a high Hartmann number.

Fig. 3: The asymptotic neutral curve $f(\kappa)$.

Fig. 4: Spatial structure of the unstable mode:

(a) vertical velocity, (b) horizontal velocity and electric current, (c) temperature perturbation. All quantities are plotted in arbitrary units.

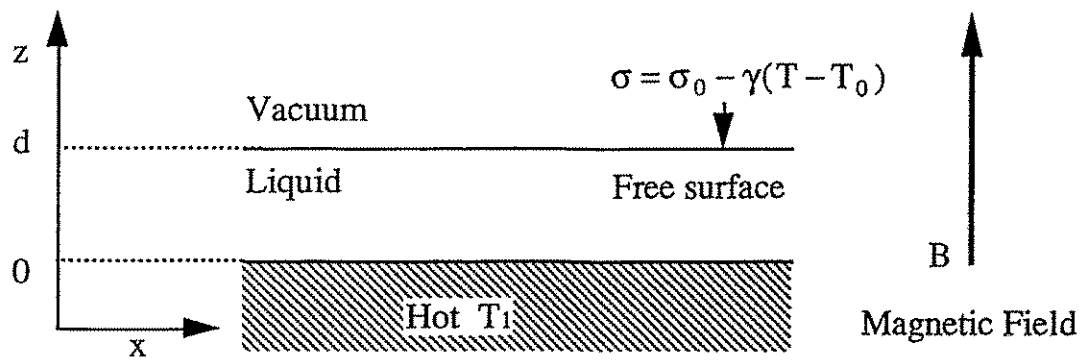
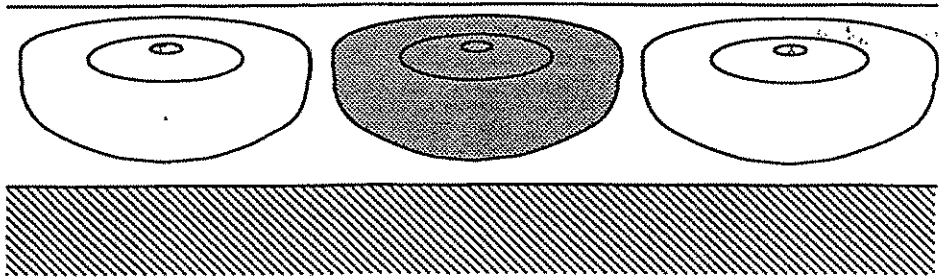


Fig 1

(a)



(b)

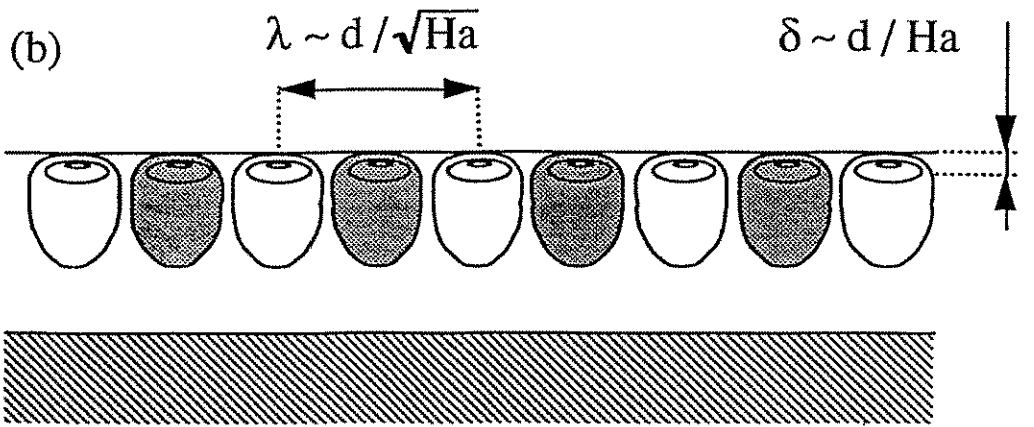


Fig 2

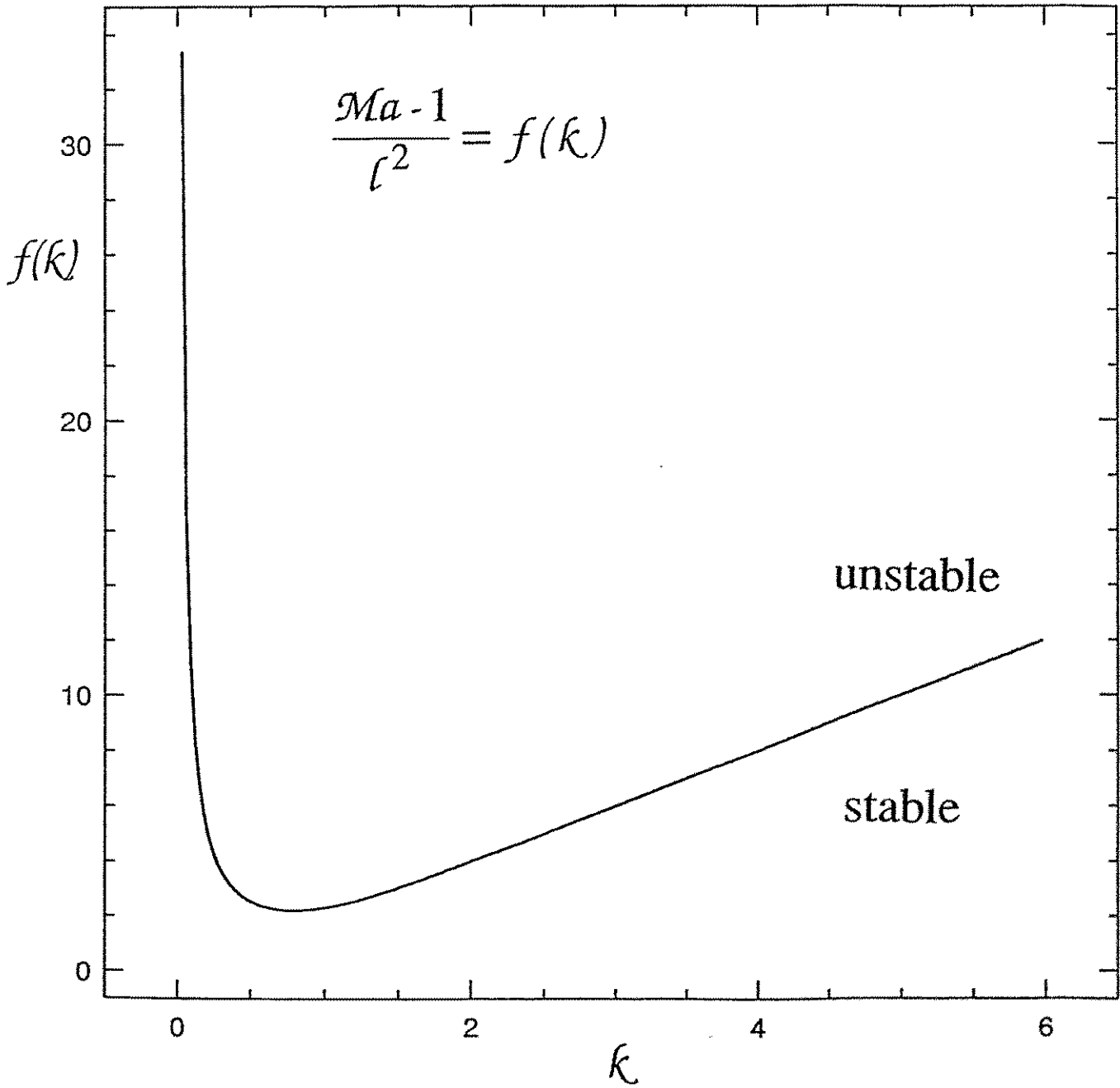
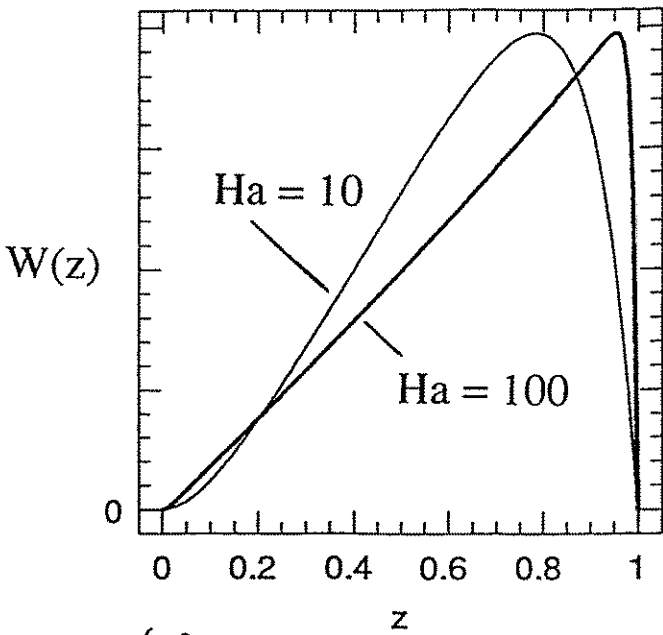
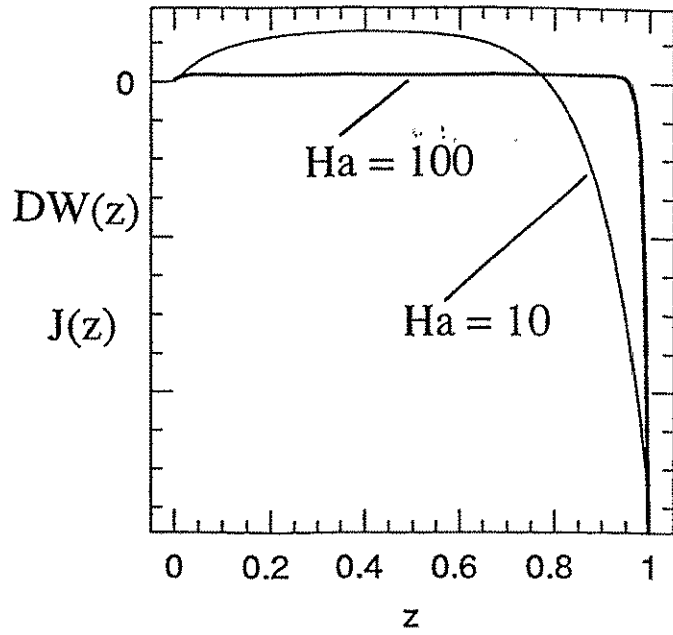


Fig 3

(a)



(b)



(c)

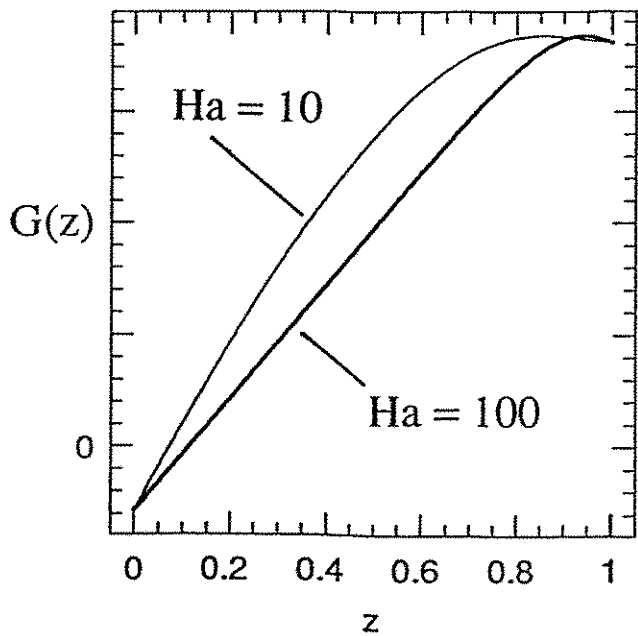


Fig 4